#493

Search for New Phenomena Using Very High Energy pp and $\bar{p}p$ Colliding Beam Devices at Fermilab

D. Cline, P. McIntyre, D. D. Reeder, C. Rubbia and L. Sulak

Department of Physics
Harvard University
Cambridge, Massachusetts 02138

Department of Physics
University of Wisconsin
Madison, Wisconsin 53706

We propose to build a detector at one of the straight sections of the Fermilab ring to detect muons and electrons produced by either pp collisions between the main ring and the energy doubler ring or $\bar{p}p$ collisions in one of the two rings. The $\bar{p}p$ option follows from the expected availability of a $\bar{p}$ injector that is being built in parallel. The detector will have the capability of observing the production and decay of the neutral and charged intermediate vector bosons.

Contents

Introduction

The technological advances represented by the energy doubler/saver ring[1] as well as the likelihood of an antiproton injector at Fermilab[2,3] open up the possibilities for colliding hadron beams at very high center of mass energy. We consider two colliding beam options in this proposal.

(a) Colliding the energy doubler/saver ring beam with the main ring beam at variable beam energies.[4]

(b) Colliding protons with the antiprotons obtained in the accumulator - cooling ring injector in either the main ring or the energy doubler ring.[2,3]

Since we expect both of these to be available within a few years at Fermilab we are encouraged to propose a single detector that can be used to obtain a first look at these ultrahigh energy collisions. In particular we concentrate on the search for the $W^{\pm}$ and W° bosons and find that the estimated luminosities and center of mass energies provided by options (a) and (b) allow a definitive search for these objects, within the most reliable expectations of present production models[5] and present models for the mass of these objects (50 - 150 GeV).[6,7]

We also concentrate on the design of a modest detector that will cause a minimum disruption of the Fermilab program when it is installed in the main ring tunnel.

The present limit on the W^{+} mass obtained from neutrino experiments in $\geq$ 20 GeV and for the W° the limit is about 10 GeV.[8] The next round of neutrino experiments at Fermilab will likely

cover the W^+ mass range from 20 - 40 GeV and perhaps go higher. With the neutrino beam provided by the energy doubler/saver it will perhaps be possible to go to 60 GeV.[1] Therefore we feel the next most immediate step in the search for the W°, W^+ and other new phenomena must be carried out with a very large jump in center of mass energy capable of search up to perhaps 150 - 200 GeV. The luminosities of options (a) and (b) will be adequate for this initial search. It is extremely fortunate that this step can be taken with rather modest devices at Fermilab within the next few years using either option (a) or (b) or both. Options (a) and (b) are also extremely complimentary in that both matter-matter and matter-antimatter collisions are to be studied. A comparison of these two kinds of collisions at these extremely high energies is very likely one of the best ways to uncover new physics. For example $\bar{p}p$ collisions should make an equal number of W^+ and W^- whereas pp collisions will produce predominately W^+. Thus a charge asymmetry is expected for large $P_\perp$ μ's that are decay products of W bosons in the pp case that is not observed in the $\bar{p}p$ case.

The final goal of these colliding beam schemes is to provide the highest center of mass energy at the largest luminosity. Using the energy doubler as a storage ring, injecting protons and antiprotons and accelerating to 1300 x 1300 GeV x GeV will give a very high center of mass energy. We estimate that luminosities in the range 10^{31}-10^{32} cm^{-2}sec may be possible with this scheme.

Since the average momentum carried by a parton in the proton or antiparton in the antiproton is $\sim 0.2|\vec{P}_p| \sim 200$ GeV/c the average center of mass energy in the parton-antiparton system is 400 GeV, very near the unitarity limit for weakly scattering point particles. Thus at this energy, for the $\bar{p}p$ system the weak interaction has become as stronge as possible. The ultimate nature of weak interactions will almost certainly be revealed by this colliding beam machine. We feel that this goal justifies the venture including the construction of an adequate detector.

2. Luminosity and C.M. Energy Estimates for the pp Option

We have considered several options for colliding the energy doubler/saver beam with the main ring beam. These options are summarized in Table 1. Basically all schemes require reversing the main ring magnets and injecting the other direction as shown schematically in Fig. 1. The main ring and energy doubler are brought together by four dipoles into a common vacuum pipe as schematically shown in Fig. 2a. Several independent luminosity estimates have been carried out.[9,10,11] In addition, T. Collins has designed a quadrupole configuration that gives a very low β interaction region.[12] The β for the interaction region and for various machine energies is shown in Fig. 3. The reason that relatively large luminosities can be obtained for this colliding beam machine is due to (1) the very small beam in the main ring and the energy doubler/saver, (2) the addition of the low β interaction region which reduces the beam size even further, (3) the possibility of bring the beams into head-on collisions. If a number of machine pulses can be stacked into the energy doubler (which has a relatively large aperature), then even higher luminosity could be obtained. The filling time of the energy doubler is expected to be the order of 100's of seconds and the time needed to reverse the main ring magnets of comparable time. The main ring beam can either be operated in a coasting mode (for the order of 10's of hours) or in a ramping mode. While the luminosities for the latter mode is reduced by about a factor of 5, this option allows the normal Fermilab physics program to be carried out at the same times of the colliding beam physics. Loss of beam due to gas scattering

has been estimated to be less than 0.3%/minute in the energy doubler/saver.[10]

Table 1

Colliding the Energy Doubler/Saver Beam

with the Main Ring Beam (p-p)

Options	Beam Energies	$S(GeV/c)^2$	Estimated Luminosity	Reference	Scheme
(A)	40 × 1000	1.6×10^5	3.4×10^{30}* $\sim 10^{29}$ 3.8×10^{29}	Cline-Richter[4] Lee Teng[9] D. Edwards[10]	Collide normal ED/S with reversed coasting ring
(B)	400 × 1000	1.6×10^6	$\sim 10^{30}$* 2.4×10^{30}	C. Rubbia[4] Lee Teng[9]	Collide normal direction ramping main ring with "reversed" energy doubler
(B')	150 × 1000	0.6×10^6	6×10^{30}*	T. Collins[11]	Collide normal direction coasting main ring with "reversed" energy doubler
(C)	400 × 400	6.4×10^5	$\sim 2 \times 10^{30}$	Lee Teng[9]	Collide normal direction ramping main ring with reversed (but unramped) ED/S

*Stacking in the energy doubler can increase these figures by a factor of 2-10.

3. Luminosity Estimate and C.M. Energy Estimate for the $\bar{p}p$ Option

The expected luminosity for this option can only be roughly estimated at this time. The basic scheme for collecting, cooling and reinjecting antiprotons into the Fermilab machine is outlined in Fig. 4. The general scheme is as follows:

1. 3.5 GeV/c antiprotons are produced by an intense, R.F. bunched beam from the main accelerator. The beam energy should be above 50 GeV but need not be above 100 GeV.
2. The $\bar{p}$'s are transported into the accumulator ring by a special transport system that matches the phase space.
3. The antiproton bunch is intially cooled in transverse and longitudinal phase space by stochastic cooling similar to that operated at the ISR.
4. The $\bar{p}$ bunch is moved into a parking orbit and another $\bar{p}$ bunch is injected. This operationg is carried out $\sim$1000 times yielding 10^{10}-10^{11} antiprotons.
5. The antiprotons are decelerated to a momentum of 350 MeV/c. Stochastic cooling keeps the beam stable.
6. An intense electron beam is turned on with the electrons traveling with the same velocity as the $\bar{p}$ and in the same direction. Approximately 1 amp/cm^2 is used. The antiproton beam phase space is cooled further to a very small value.

7. The antiproton beam is accelerated up to 9.0 GeV/c.
8. The antiprotons are extracted into a transport system and carried back to the main ring.
9. The $\bar{p}$ are injected into the main ring and a pulse of 5×10^{10} - 5×10^{12} protons are obtained in the main ring and all accelerated up to 50 GeV/c.
10. For higher luminosity ($\sim 10^{30}$-10^{31} $cm^{-2}sec^{-1}$) requirements some additional R. F. bunching is required.
11. The p and $\bar{p}$ are accelerated to 200 GeV and collide at one or more long straight sections.

The estimated range of luminosity of this machine is given in Table II. The scheme for colliding the beams in the common interaction with the pp option is shown in Figs. 2b and 2c. For the 150 × 150 GeV/c option in Table II the main ring is used for the accelerator and storage ring. 150 GeV/c is then chosen because of the excellent low β interaction configuration (Fig. 3) and because the power supplies in the main ring can be turned on D.C. at this energy. For the 1000 × 1000 GeV/c option the energy doubler stores the beam and the main ring continues to operate normally. In this normal operation we imagine that the cooling ring would be continuously refilled thus allowing continuous operation of the $\bar{p}p$ ring. If the energy doubler/saver has a good vacuum ($\sim 10^{-9}$ torr) this mode of operation would allow very long storage times (> 50 hours) and for the possibility of additional stacking of $\bar{p}$'s into the ring. The luminosity could then be increased perhaps to the range 10^{31} $cm^{-2}sec^{-1}$. This luminosity coupled with 2000 GeV in the $\bar{p}p$ c.m. system would undoubtedly provide the most sensitive search for W bosons, perhaps as sensitive as 1000 × 1000 GeV pp

Table II

Colliding Protons and Antiprotons

Options	Beam Energies	S $(GeV/c)^2$	Estimated Luminosity	Reference
(A')	250 × 250	2.5×10^5	5×10^{29}+	Cline, McIntyre, Rubbia[2]
(A)	150 × 150	0.9×10^5	$10^{29} - 10^{30}$	D. Cline et al.[3]
(B)	1000 × 1000	4×10^6	$10^{31} - 10^{32}$*	D. Cline et al.[3]

*Stacking $\bar{p}$'s in the energy doubler can increase the luminosity by up to another factor of 10.

+This scheme is now expected to give a luminosity of $\sim 10^{31} cm^{-2} sec^{-1}$.

colliding rings with luminosities of one or two orders of magnitude greater. Thus the $\bar{p}p$ option combined with the energy doubler/saver operated as a storage ring would compete favorably with any planned colliding beam project.

We now outline three more specific schemes for obtaining the luminosity reported in Table II. These schemes are further discussed in the cooling ring proposal. The salient features and requirements of each scheme is given here.

Scheme A

1. The main ring is operated to accelerate protons to 50 GeV/c. At 50 GeV/c the protons are R.F. bunched rapidly by turning on a lower frequency cavity in a programmed fashion and then turning the 50 mHz cavity back on. Bunches with 2×10^{12} protons are obtained (1113 bunches are collapsed into $\sim$25 bunches).
2. The bunched proton beam is extracted, and produces a short bunch of $\bar{p}$'s that are injected into the accumular-cooling ring.
3. The bunched $\bar{p}$ beam is out of phase with the previously accumulated and coasting $\bar{p}$'s; it thus does not disturb the parked beam.
4. This operation produces 3×10^{7} $\bar{p}$/pulse.
5. The next R. F. bunched proton beam is made ready, the time available for the R. F. bunching is approximately that needed to "cool" the previous $\bar{p}$ bunch in the cooling ring a few seconds. This operation is carried out 1000 times giving 3×10^{10} $\bar{p}$'s.

6. The $\bar{p}$'s are cooled and then injected back into the main ring at 9.0 GeV/c.
7. The main ring is filled with protons from the boostor and along with the $\bar{p}$ bunch all are accelerated to 50 GeV/c.
8. At 50 GeV/c the protons are R. F. bunched into bunches of 5×10^{12} protons. The $\bar{p}$'s are unaffected since they were all in one bunch to start with.
9. p and $\bar{p}$'s are accelerated to 200 GeV/c and collide in the main ring.
10. The luminosities for this option is shown in Fig. 5 ($L \sim 10^{31} cm^{-2} sec^{-1}$).

Scheme A'

This scheme is the same as A except

1. The protons are <u>not</u> additionally R. F. bunched in the main ring. The parked antiproton beam is tightly R. F. bunched into one bucket.
2. The effective number of protons that are available to produce $\bar{p}$'s is determined by

$$\left(\frac{\text{diameter of small ring}}{\text{diameter of large ring}}\right) \times 5 \times 10^{13}$$

3. The injected $\bar{p}$'s fill all the buckets but the one with the coasting parked $\bar{p}$ beam.
4. This operation continues for 6000 pulses and 7×10^{10} $\bar{p}$'s are collected.
5. The $\bar{p}$'s are injected into the main ring accelerated along with the normal proton bunches up to 200 GeV/c.

Most of the proton buckets are bunched out of the machine. Thus 7×10^{10} $\bar{p}$'s collide with 5×10^{10} protons. The luminosity, given in Fig. 5 is $\sim 5 \times 10^{29}$ $cm^{-2}sec^{-1}$.

Scheme B (High Luminosity, high C. M. energy option)

This scheme has three basic elements.

1. The protons are partially R. F. bunched to obtain 5×10^{11} protons/bunch above 50 GeV/c.
2. The bunched proton beam along with multiturn injection into the little ring produces 3×10^{7} $\bar{p}$'s/ pulse. Multiturn injection may require a second cooling ring for the parked antiprotons adjacent to the "accumulator ring".
3. The antiprotons injected back into the main ring are accelerated up to 400 GeV/c and injected into the energy doubler. Protons are injected from the booster accelerated to 50 GeV/c, R. F. bunched into 5×10^{11} protons/ bunch accelerated up to 400 GeV/c and injected into the energy doubler. The protons and antiproton bunches are accelerated to 1000 GeV/c and collide head on. The estimated luminosity is $\sim 10^{32} cm^{-2} sec^{-1}$ (see Fig. 5).
4. The main ring continues to operate normally, filling the cooling ring, additional $\bar{p}$ and p bunches are injected from time to time with the luminosity growing accordingly.

In scheme B the energy doubler is used as a $\bar{p}p$ storage ring. If the energy doubler has a good vacuum ($\sim 10^{-9}$ Torr) it will be a nearly ideal storage ring at these extremely high energies.

We are certain other schemes can be imagined that give more or less the same luminosity estimates as A', A, B. We illustrated these schemes only to indicate that the availability of an anti-proton source for the Fermilab machine will almost certainly lead to a colliding beam device of adequate luminosity and the need for the detector proposed here.

4. Rates and Experimental Signature for W Production

The past ten years have seen remarkable progress in the understanding of weak interactions. First there is the experimental discovery of $\Delta S = 0$ weak neutral currents, which when contrasted with the previous limits on $\Delta S = 1$ neutral current decay processes leads to the suggestion of additional hadronic quantum numbers in nature. Strong evidence now exists for new hadronic quantum numbers that are manifested either directly or indirectly. The experimental discoveries are complemented by the theoretical progress of unified gauge theories. These developments lead to the expectation that very massive intermediate vector bosons (50-100 GeV/c^2) may exist in nature. The search for these massive bosons require three separate elements to be successful: a reliable physical mechanism for production, very high center of mass energies, and an unambiguous experimental signature to observe them. The center of mass energies for the pp or $\bar{p}p$ option as discussed previously cover the range of 300-2000 GeV, which is kinematically high enough energy to produce intermediate bosons in the mass range of 50-200 GeV. However, the production cross section is very likely to depend on the mass of the W and the available center of mass energies, thereby determining the minimum luminosity for the machine.

We therefore first turn to the production process (and attempt to estimate the production cross section. We concentrate on neutral bosons because of the extremely simple experimental signature and because production is largely dominated by a single production resonant pole in the particle-antiparticle cross section. The best production reaction would of course be

$$e^+ + e^- \rightarrow W^\circ \rightarrow \begin{cases} e^+ + e^- \\ \mu^+ + \mu^- \\ \text{hadrons} \end{cases}$$

where a sharp resonance peak is expected for $2E_{e^+} = 2E_{e^-} = M$. In the Breit-Wigner approixmation near its maximum we get:

$$\sigma(e^+e^- \rightarrow W^\circ) \simeq \frac{3}{4}\pi\lambda^2 \frac{\Gamma_i \Gamma}{(2E - M)^2 + \frac{\Gamma^2}{4}}$$

where Γ_i, Γ are the partial width to the initial e^+e^- state and the total width, respectively. The decay widths into e^+e^- (and $\mu^+\mu^-$) pairs can be calculated in the first order of the semi-weak coupling constant: $\Gamma_{e^+e^\pm} \cong \Gamma_{\mu^+\mu^-} = 1.5 \times 10^{-7} M_W^3$ (GeV). For M = 100 GeV, $\Gamma_{e^+e^-} \simeq 150$ MeV, which is surprisingly large. The total width is related to the above quantity by the branching ratio $B_{e^+e^-} = \Gamma_{e^+e^-}/\Gamma$ which is unknown. Crude guesses based on quark models suggest $B_{e^+e^-} \simeq 1/10$, giving $\Gamma = 1.5$ GeV or $\Gamma/2E = 1.5\%$ for M = 100 GeV/c^2. At the peak of the resonance, $\sigma(e^+e^- \rightarrow W^\circ, 2E = M) = 3\pi\lambda^2 B_i \simeq 2.10^{-31}$ cm^2. In the Weinberg-Salam model the W° mass is now estimated to be $M_W > 84$ GeV.[6,7] This mass is outside the reach of presently planned new generation of e^+e^- storage rings.

A more practical production process is the one initiated by proton-antiproton collisions:

$$p + \bar{p} \rightarrow W^\circ + (\text{hadrons})$$

which, according to the quark (parton) picture, proceeds by a reaction analog to (1), except that now incoming e^+ and e^- are replaced with q and $\bar{q}$. Strong support to the idea that W's are directly coupled to spin 1/2 point-like constituents comes from

neutrino experiments and from semi-leptonic hadron decays. Furthermore neutrino experiments provide the necessary structure functions and have set limits (> 20 GeV) on any nonlocality in the parton form factor.[8] The main difference with respect to e^+e^- is that now the kinematics is largely smeared out by the internal motion of q's and $\bar{q}$'s. The average center of mass energy squared of the $q\text{-}\bar{q}$ collision is roughly

$$\langle S_{q\bar{q}} \rangle \sim S\langle x_q \rangle_p \langle x_{\bar{q}} \rangle_{\bar{p}}$$

where S is the center of mass energy squared of the $\bar{p}p$ system and $\langle x_q \rangle_p$ ($\langle x_{\bar{q}} \rangle_{\bar{p}}$) is the mean fractional momentum of q's ($\bar{q}$'s) in the proton (antiproton). From the neutrino measurements and $\langle x_q \rangle_p = \langle x_{\bar{q}} \rangle_{\bar{p}}$ we find $\langle S_{q\bar{q}} \rangle \sim 0.04\ S$. For $M = 100\ \text{GeV}/c^2$ this suggests $S \geq 2 \times 10^5\ \text{GeV}^2$ of $\sqrt{S} \geq 450$ GeV. The production cross section can be evaluated by folding the (narrow) resonance (2) over the q and $\bar{q}$ momentum distributions:

$$\sigma(q\bar{q} \to W^\circ \to \mu^+\mu^- \text{ or } e^+e^-) = 3\pi\lambda^2 \frac{\Gamma_{q\bar{q}}}{\Gamma} \cdot \frac{\Gamma_{\mu\mu}}{\Gamma} \cdot \frac{dN}{dE}(E = M) \cdot 2\Gamma \qquad (3)$$

where dN/dE is the probability (per unit of energy) of finding a $q\bar{q}$ collision with center of mass energy E, and other symbols have the same meaning as in (2). Note that $(\Gamma_{q\bar{q}}/\Gamma) \simeq 0(1)$ is a model-dependent parameter. The resultant cross section is $\sigma(p\bar{p} \to W^\circ + \text{hadrons} \to \mu^+ + \mu^- + \text{hadrons}) \simeq 6\pi\lambda^2 \frac{\Gamma_{q\bar{q}}}{\Gamma} \frac{dN}{dE}(E = M)$. $\Gamma_{\mu\mu} \cong 10^{-32}$ cm^2. A similar cross section is expected for the charged boson. The numerical value is given for $M = 100\ \text{GeV}/c^2$, $\sqrt{S} = 500$ GeV and $(\Gamma_{q\bar{q}}/\Gamma) = 1/2$. This derivation of the cross section exposes the basic simplicity of the assumptions and gives the order of magnitude of the expected cross section. More sophisticated calcula-

lations give similar results.[5]

We note that calculations of W^o and W^+ production in proton-proton collisions are very uncertain in contrast to the present one due to the apparent small antiparton content in the nucleon and the unknown x distributions of this component.[5] This leads to a great uncertainty in the production cross section and therefore the energy needed to reliably search for the boson.[5] The expected cross section and the theoretical uncertainty for a 100 GeV boson are shown in Fig. 5. Folding in a branching ratio for $W \to \mu + \nu$ of 10% we can estimate the luminosity needed to observe 1 W production in 10 hours as showing in Fig. 6. Note that for $\bar{p}p$ option (B') the luminosity and high center of mass energy would give about 1 W/hr even in the realistic model.

We turn now to the question of the experimental observation. The cleanest experimental signature for the program outlined here is:

$$\bar{p} + p \to W^o + \text{hadrons} \quad \text{or} \quad p + p \to W^o + \text{hadrons}$$
$$\hookrightarrow \mu^+ + \mu^- \qquad\qquad \hookrightarrow \mu^+ + \mu^-$$
$$\hookrightarrow e^+ + e^- \qquad\qquad \hookrightarrow e^+ + e^-$$

with the observation of a peak in the $\mu^+\mu^-$ or e^+e^- invariant mass spectrum. Electromagnetic production of $\mu^+\mu^-$ (e^+e^-) pairs is expected to be suppressed by a factor of $\approx (\alpha^2/G^2M_W^4)$. Note that a similar suppression is expected to hold for any hadronic vector meson. Note also that the production and decay of charged vector bosons is more problematic since the decay sequence

$$\bar{p} + p \to W^+ + X \quad \text{or} \quad p + p \to W^+ + X$$
$$\hookrightarrow \mu^+ + \nu_\mu \qquad\qquad \hookrightarrow \mu^+ + \nu_\mu$$
$$\hookrightarrow e^+ + \nu_e \qquad\qquad \hookrightarrow e^+ + \nu_e$$

leads to one muon (electron) and a missing neutrino which is difficult if not impossible to detect. In many previous discussions it has been assumed that the W^+ would be produced with very little transverse momentum with respect to the incident beam direction and therefore the transverse momentum of the decaying μ would exhibit a sharp peak at $p_{\mu\perp} \sim M_W/2$. Present evidence in case of the production of massive strongly interacting vector bosons (i.e., J/ψ) indicate that the parent is produced at relatively large $p_\perp$ and therefore the Jacobian peak is largely smeared out. There is no obvious reason why the production of massive intermediate vector bosons should not follow the same behavior. Without a sharp structure in the p_μ distribution, a crucial experimental signature for the W^+ is absent. Thus it is of extreme importance to produce a large numbers of charged W's in either the pp or $\bar{p}p$ option if the charged W is to be detected. We believe this requires very high C.M. energy and an adequate luminosity (pp(option B') or $\bar{p}p$ (option b).

Because of a lack of completely reliable production cross section numbers and since we do not really know the expected mass of the W^+ or W° bosons, the search for these objects must be carried out in a very broad sweep with a large jump in the center of mass energy over present searches. (Perhaps a factor of at least 10 is needed to be safe.) If a narrow approach is taken, focussing on a small mass range or, a particular production process or a specific decay mode, the W could be missed. We, therefore, feel that a search must be conducted with both pp and $\bar{p}p$ colliding beams, and with the highest luminosity available and emphasizing both μ and e decay

modes. Furthermore, both W° and W^{+} must be searched for. This philosophy governs the two major pieces of equipment we are proposing to build, the $\bar{p}$ cooling ring and the experimental detector. It is again extremely fortunate that such a program could be carried out in the next few years at Fermilab.

In the remainder of this proposal we describe a minimal detector that is capable of observing the $W^{\pm}$ or W° production. The background estimates assume that either the options pp(B') or $\bar{p}p(A')$ are the case.

Table III

Estimates Rates for W Production and Decay

for the Various Colliding Beam Configurations

	Process	Colliding Beam Option	Mass of W	Estimated Number of Events/hr	Remarks
	$\bar{p} + p \rightarrow W^{\circ} + X$	$\bar{p}p$ (A')	100	1 - 10	Production estimates most reliable
1)	$\rightarrow \mu^{+} + \mu^{-}$	$\bar{p}p$ (B)	100	10 - 100	Experimental signature reliable
2)	$\rightarrow e^{+} + e^{-}$				
	$\bar{p} + p \rightarrow W^{+} + X$	$\bar{p}p$ (A')	100	1 - 10	Production mechanism reliable
3)	$\rightarrow e + \nu$	$\bar{p}p$ (B)	100	10 - 100	Experimental signature not reliable
	$p + p \rightarrow W^{+} + X$	pp (A)	100	0.1	Production dependent on antiparton momentum spectrum
	$\rightarrow e + \nu$	pp (B)		$\sim$0.3	
		pp (B')		$\sim$1	Production estimates less dependent on antiparton momentum spectrum
4)	$p + p \rightarrow W^{\circ} + X$	pp (B')		$\sim$1	

Experimental Apparatus

We have designed a detector to look for the most characteristic signature of $W^{\pm}$ or W° production, high $p_{\perp}$ leptons. The design presented here follows closely that developed by the 1975 ISABELLE summer study. It can be used for either single lepton or dilepton searches and may have sufficient solid angle to be able to deduce the existence of a neutrino, from the $W^{\pm}$ decay, via the imbalance in transverse momentum. In addition, since this detector will be exploring a new region of physics, we felt that versatility was desirable and therefore it was designed with the capability of identifying both electrons and muons.

The general configuration of the electron detector is shown in Figs. 8, 9 (the inner detector). The purpose of the inner section of the detector is to detect the electron from the W decay while at the same time reject with good sensitivity the presence of a hadron. The electron identifier in conjunction with the calorimeter should, at $p_{\perp} > 10$ GeV/c, discriminate against pions at the level of 10^{-4} while still detecting most of the leptons. This high rejection level was chosen to protect ourselves from "surprises" at very high energies. The muon detector (outer detector in Fig. 8, 9) is discussed later.

The e-π separation of approximately 10^4 to 1 can be achieved by having an electron identifier which can detect leptons with less than 1% pion background while the calorimeter, occupying the middle section of the detector, can achieve another factor of 100 in the hadron-electron separation. The calorimeter front end has maximum sensitivity to electromagnetic showers, while the rest of the module is optimized as a hadronic calorimeter. The outer sec-

tion of the detector, the muon identifier, is composed of magnetized iron. This should allow a measurement of muon momentum to an accuracy of roughly 18%.

The acceptance of the detector depends to some extent on whether it is being used with p-p colliding beams at 150 × 1000 (pp(B')) GeV^2 (γ_{cm} = 1.5) or $\bar{p}$-p colliding beams at 150 × 150 GeV^2 (γ_{cm} = 1)($\bar{p}$p(A)). In either case it has full acceptance for c.m. angles greater than 45°, providing 3π ster. solid angle acceptance. There are end caps composed of magnetized calorimeters, in order to catch missing transverse momentum.

Figure 10 shows the $\pi^{\pm}$ spectrum at angles $\geq$ 40° in the p-p and $\bar{p}$-p colliding beams. These particles almost all have p of a few hundred MeV, and can present a serious problem both by making a high accidentals rate in the inner detector chambers and counters, and by simulating an $e^{\pm}$ when they are associated with a high $p_{\perp}\pi^{\circ}$ in traversing the electron detector. We remove a considerable portion of this problem by placing a superconducting solenoid around the entire length of the interaction region. All particles of $p_{\perp}$ < 220 MeV/c are contained in the beam pipe, and particles of $p_{\perp}$ < several GeV can be easily distinguished in the characteristic back-to-back $\ell^+\ell^-$ topology by the closest distance of approach of the tracks extrapolated to the interaction diamond.

Electron Identification Module

1. Transition Radiation Detectors Detection of the transition radiation produced when a relativistic particle passes through an abrupt interface between to materials of different electron densities has been proven to be a practical and very powerful tool for the detection of particles with high γ [$\gamma = (1 - \beta^2)^{-1/2}$]. We propose to use this technique as the primary element of the electron identifier.[13] An extremely efficient transition radiator that has been constructed consisted of stacks of a large number of thin lithium foils followed by a xenon-gas filled MWPC to detect the x-rays from the radiator.[13] Such a radiator-detector system has been extensively tested and is being used for electron identification in an experiment at the ISR with a very similar geometry to the one proposed here.

We determine the optimal performance of our electron identifier by extrapolating the performance of the ISR detector to our region of kinematic interest. The ISR detector is optimized for electrons in the 1 to 5 GeV/c range, while our detector needs to be optimized for the detection of electrons in the 10 to 50 GeV/c range, while providing good pion rejection in this region. The total energy radiated from a single foil increases linearly with γ so that in principle the x-ray intensity should increase linearly with the momentum of the particle. At particle energies above a few GeV/c, the limitation in the π-e separation is the Landau tail in the ionization energy deposited by the pions in the xenon MWPC. While an increase in the momentum of the pions increases the ionization energy loss due to the relativistic rise ($\sim$30% increase), we

would expect a much larger increase in the x-ray yield (a factor of 10). Hence overall we would expect a large improvement in the π-e separation at higher energies. In practice, however, there are two factors which severely limit this improvement. One is the fact that as γ increases, the maximum frequency of the emitted x-ray radiation increases linearly, while the intensity at a particular frequency only increases logarithmically. Hence most of the additional energy comes in the form of high energy x-rays (> 20 keV). Unfortunately these high energy x-rays are hard to detect with MWPC because the total photon cross section falls as a high power of the incident x-ray energy. The other limitation is due to the saturation in the production of x-rays due to existence of limiting distances between surfaces called formation zones.

The detector is optimized for the energy regime between 10 and 50 GeV, by using a thickness of lithium foils of 1.25 mils and a foil separation of 20 mils. With this geometry we calculate that 400 foils will yield a detected x-ray intensity 30% larger than the ISR detector. This is sufficient to offset the 30% increase in the hadron energy deposition. In addition, the transition radiator can achieve better pion rejection if we lower slightly its electron detection efficiency. For two units, the levels become 2.5×10^{-3} for pions and .80 for electrons.

2. Design Description. The electron detector will consist of a set of Li foil transition radiators (TR). In order to get better than 100 to 1 electron to pion separation, the energy deposited by the x-rays from two stacks of transition radiators is sampled.

Each stack will consist of 400 1.25 mil Li foils separated by 20 mils, making each stack about 22 cm long. The spacing between foils will be accurately maintained by having dimples in the foils themselves. The boxes made out of sheet metal will be supported from the top and outer side with aluminum channel. In addition there will be a thin metal plate at the bottom of each stack to support the weight and a mylar window at the top thin enough to allow the x-rays to get through.

Immediately outside the beam pipe is a 2 m long, 1.3m diameter superconducting solenoid, with a 1.5T enclosed field. This provides a means of suppressing low $p_\perp$ pions. Inside the solenoid is a set of 2 stereo proportional wire chambers (PWC) in a hexagonal arrangement around the pipe. These are followed by 6 TR units around the pipe as shown in Fig. 8, 9. One Xe chamber will measure the x-ray energy from the electrons. Next there is a thin gold foil to stop the x-rays and another PWC to measure the ionization energy from the track coming through to make sure it is a minimum ionizing track. This group is followed by 24 TR units, four in each sextant as shown in Figs. 8 and 9. These are subdivided because for the outer TR the dimension of the foils would be 77 × 156 cm^2 and they could not support their own weight. This last unit is followed by a Xe PWC to sample the x-ray energy from this last unit.

The PWC will have 2 mm wire spacings except for the innermost ones which will be 1 mm. The innermost chambers will have 200 wires each leading to a total of 2400 readout wires. They cover a length of 3 m. The middle chambers have 220 readout wires each giving

rise to a total of 2640 readout wires. The outermost chambers have 385 readout wires each or a total of 2310 readout wires. This gives rise to a total of 5550 readout wires. Each wire will be read out at both ends to get rough track coordinates along the beam direction by using the method of current division. The innermost chambers will be run in the mode that will maximize its fast response since they are in a "hostile environment". The other chambers farther out will use Xe as the detecting gas.

An electron signal will consist of a charged track that gives a signal in every chamber, a large signal in chambers 3 and 5, and a minimum ionizing particle signal in chamber 4. The electron pion separation suffers because the ionization loss of the pions has a Landau tail which gives an energy deposition as large as that of the x-rays from the TR stack.

Electron-Hadron Calorimeter

The middle section of the detector is a calorimeter, composed of two cylindrical units, one optimized for electrons and the outer one for hadrons. Figure 8 shows the calorimeter position relative to the inner section, described previously.

For the electron calorimeter we can adopt either one of the two options. The first, more conservative option would be a system of "γ-catchers" similar to the ones designed, tested and being used in the ν experiment E310. These consist of 20 radiation lengths of Pb-liquid scintillator shower counters with 5 mm sampling.

We are currently developing a more appealing alternative, based on liquid Ar calorimetry. The active medium, liquid Ar, a condensed material (1.4 g/cm^3) which does not attack electrons,

has a high electron mobility (5 mm/μsec at 1 kV/mm). We are developing a detector in which wires are supported in the liquid Ar as in a standard PWC, and a stable column of gas is formed around each wire using the phenomenon of film-boiling. The resulting gas multiplication would much simplify the electronics needed to measure energy deposition.

b) μ Detection

The detector configured for μ and e detection is shown in Fig. 8, 9. 2 M of steel is used to identify the muon. The momentum resolution of a) the central solenoid, b) the first gap (1m) in the μ spectrometer, and c) the second gap (2m) are shown in Fig. 11a as a function of p_μ. The expected punchthrough for pions with $P_\perp > 25$ GeV/c is less than $\sim 10^{-3}$ per pion (see Fig. 11b and a conservative estimated yield of such pions is less than 10^{-7} per pp or $\bar{p}p$ (Fig. 10) collision, yielding $< 10^{-10}$ effective punchthrough hadrons per collision. The expected yield of muons from W production is at least two orders of magnitude higher. Punchthrough and $\pi \to \mu$, $K \to \mu$ decay backgrounds are expected to be negligible for the dimuon signature of W° production. The effect of punchthrough is attenuated by sampling the 6 interaction length calorimeter and suppressing events in which a candidate μ interacts. The residual punchthrough should approach the limit $e^{-6} = 10^{-3}$ before the magnet, and be further reduced by a similar factor in traversing the 2m of steel. The main virture of using muon identification for W production is the possibility of picking up a signal of single or dimuons in the presence of very high multiplicity hadronic final states. Such final states could cause confusion in the electron detector. The major drawback is the poor momentum resolution $\delta p/p \sim 18\%$ for single μ's.

c. Tunnel Modification Needed for the Detector

We have outlined two detectors, one capable of electron detection and electron energy measurement and another that can be used to detect both electrons and muons. The former detector is the minimal detector that will be useful for the W search whereas the latter would insure a broad search for other new phenomena.

Both of these detectors require modifications of the existing tunnel in the vicinity of the straight sections Do, Eo or Co. As an example of a possible tunnel modification we show Fig. 12. The minimum size experimental area needed for the electron detector. The modified tunnel modification for the muon-electron detector is shown in Fig. 13. A provision for some crane coverage is probably also necessary.

6. Summary

We have outlined a scheme to produce and study the collisions of very high energy pp and $\bar{p}p$ beams at Fermilab. The luminosity may be obtained by multiple stacking in the energy doubler (pp(option B')), by using longer $\bar{p}$ collection times in the ($\bar{p}p$(option A)) or multiple $\bar{p}$ stacking in the energy doubler ($\bar{p}p$(option A)) or multiple $\bar{p}$ stacking in the energy doubler ($\bar{p}p$(option B)). A summary of the luminosity vs. center of mass energy colliding beam devices proposed here and those proposed elsewhere is shown in Fig. 14. We also note the luminosity required to produce and detect 1W/hr in Fig. 14.

A preliminary detector has been designed. We feel that this is the minimal that will be useful for the W searches. A substantial increase in the tunnel size at one of the straight sections is required. We also urge the laboratory to maintain at least two free straight sections that are 180° apart in the ring for the $\bar{p}p$ colliding beam options.

The time scale for constructing the detector is about two years after given approval by the laboratory provided adequate funding is available.

The strongest rationale for building these devices is the search for the intermediate vector boson since we now will have sufficient energy in the center of mass and sufficient luminosity along with reliable production cross section estimates and good experimental signature to be certain to observe these objects, if they exist. This justifies the venture and the need for a

very large step in energy. We illustrate the magnitude of this step in Fig. 15 where the various options are contrasted with the mass range that is presently being studied in neutrino collisions. The cost of the tunnel modification and the transfer line to inject protons backward into the main ring are the only appreciable additional investments the laboratory need make for the ED/s colliding with the main ring. Any colliding beam device requires a detector of the kind discussed here and this cost would be common to all schemes.

References

1. Energy doubler/saver proposal, 1975.
2. Producing Massive Neutral Intermediate Vector Bosons with Existing Accelerators, C. Rubbia, P. McIntyre and D. Cline, submitted to Phys. Rev. Letters.
3. Proposal to build an Antiproton Injector for the Fermilab Machine, D. Cline et al., submitted to Fermilab, May, 1976.
4. Private communications from D. Cline, B. Richter and C. Rubbia to R. R. Wilson (1975).
5. Drell-Yan, Phys. Rev. Letters 25, 316 (1970), Pakvasa, Parashar, and Tuan, Phys. Rev. D10, 2124 (1975), S. M. Berman, Bjorken, Kogut, Phys. Rev. D4, 3388 (1971), G. Altarelli et al., Nucl. Phys. B92, 413 (1975) and R. B. Palmer, Paschos, Samios and Wang, BNL preprint 20634.
6. S. Weinberg, Phys. Rev. Letters 19, 1264 (1967).
7. A. Salam in Elementary Particle Physics (edited by N. Svortholm, Almquist and Wiksells, Stockholm, 1968), p. 367.
8. A. Benvenuti et al., "Test of Locality of the Weak Interaction in High Energy Neutrino Collisions", to be submitted to Phys. Rev. Letters (March 1976).
9. L. C. Teng, talk at an informal meeting, January 1976.
10. D. Edwards, "Remarks on Colliding the Main Ring and Energy Doubler Beams", Internal Fermilab note.
11. T. Collins, private communication.
12. T. Collins, "Easy Low-Beta for the Main Ring", TM649-0400.
13. J. Fisher, S. Iwata, V. Radeka, C. L. Wang and W. J. Willis, BNL 20063, NIM (in press).

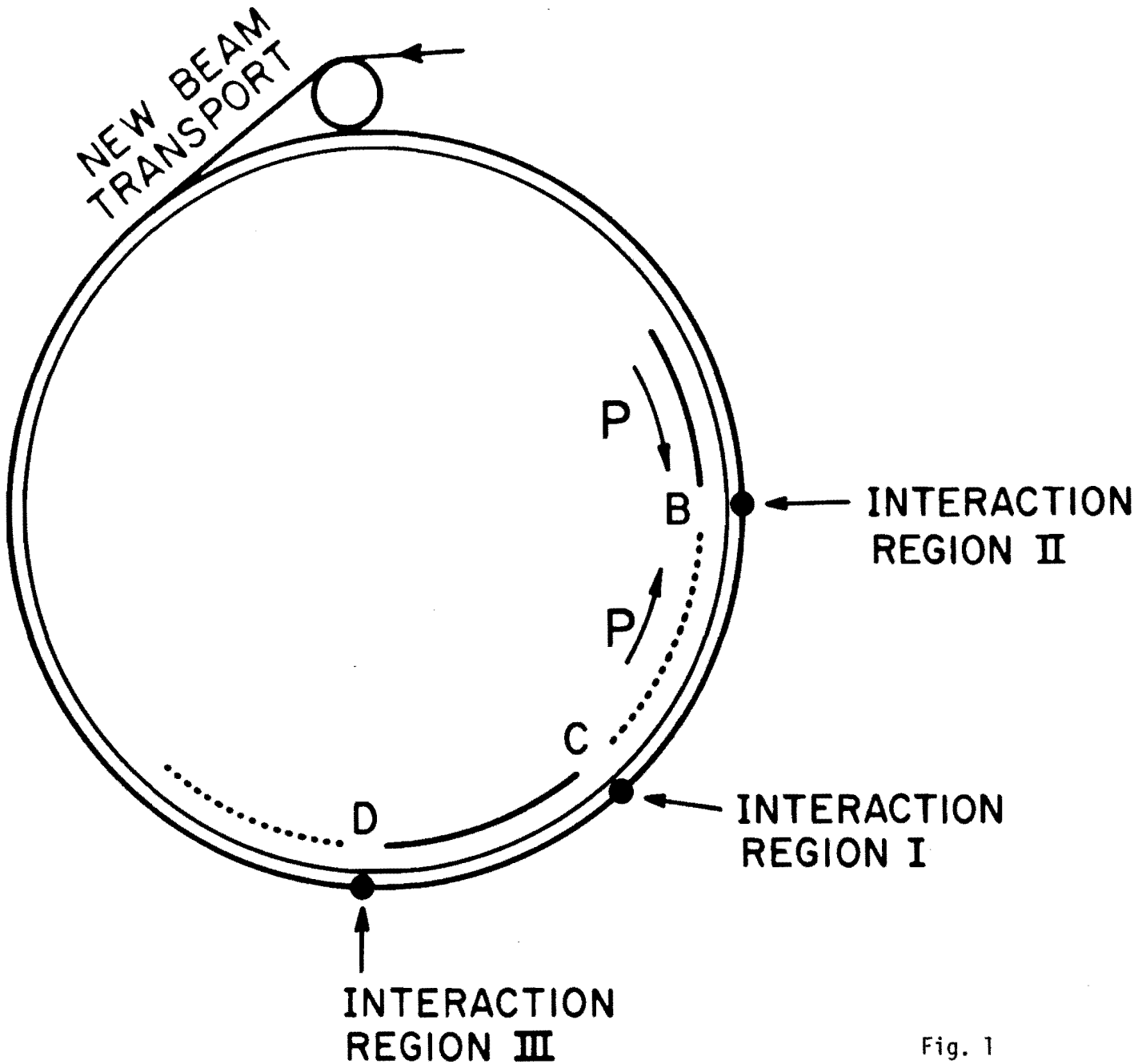
NEW BEAM TRANSPORT
P
B
INTERACTION REGION II
P
C
D
INTERACTION REGION I
INTERACTION REGION III

Fig. 1

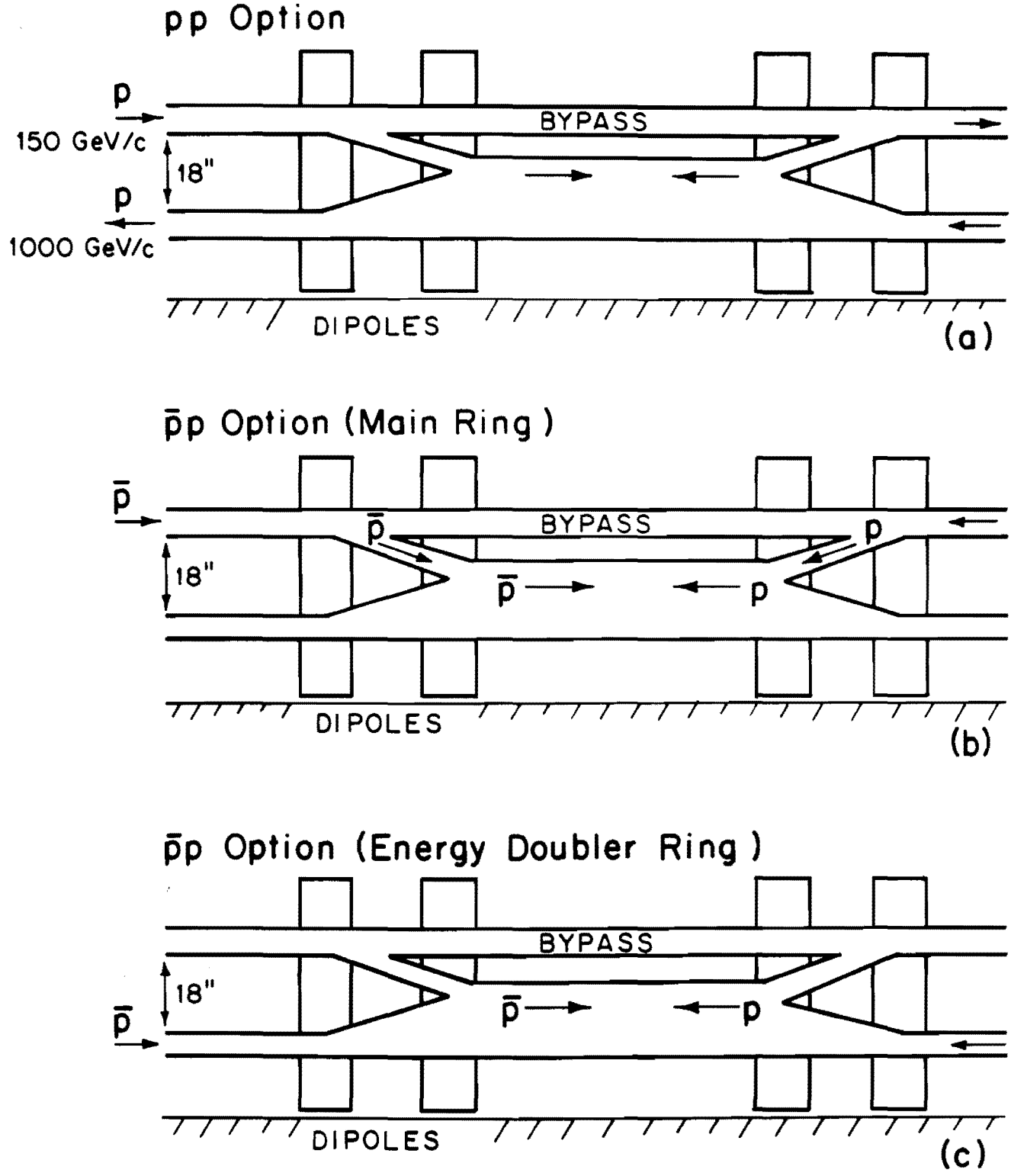
pp Option
p
150 GeV/c
18"
p
1000 GeV/c
BYPASS
DIPOLES
(a)
p̄p Option (Main Ring)
p̄
18"
p̄
BYPASS
p
p̄
p
DIPOLES
(b)
p̄p Option (Energy Doubler Ring)
BYPASS
18"
p̄
p̄
p
DIPOLES
(c)

Fig. 2

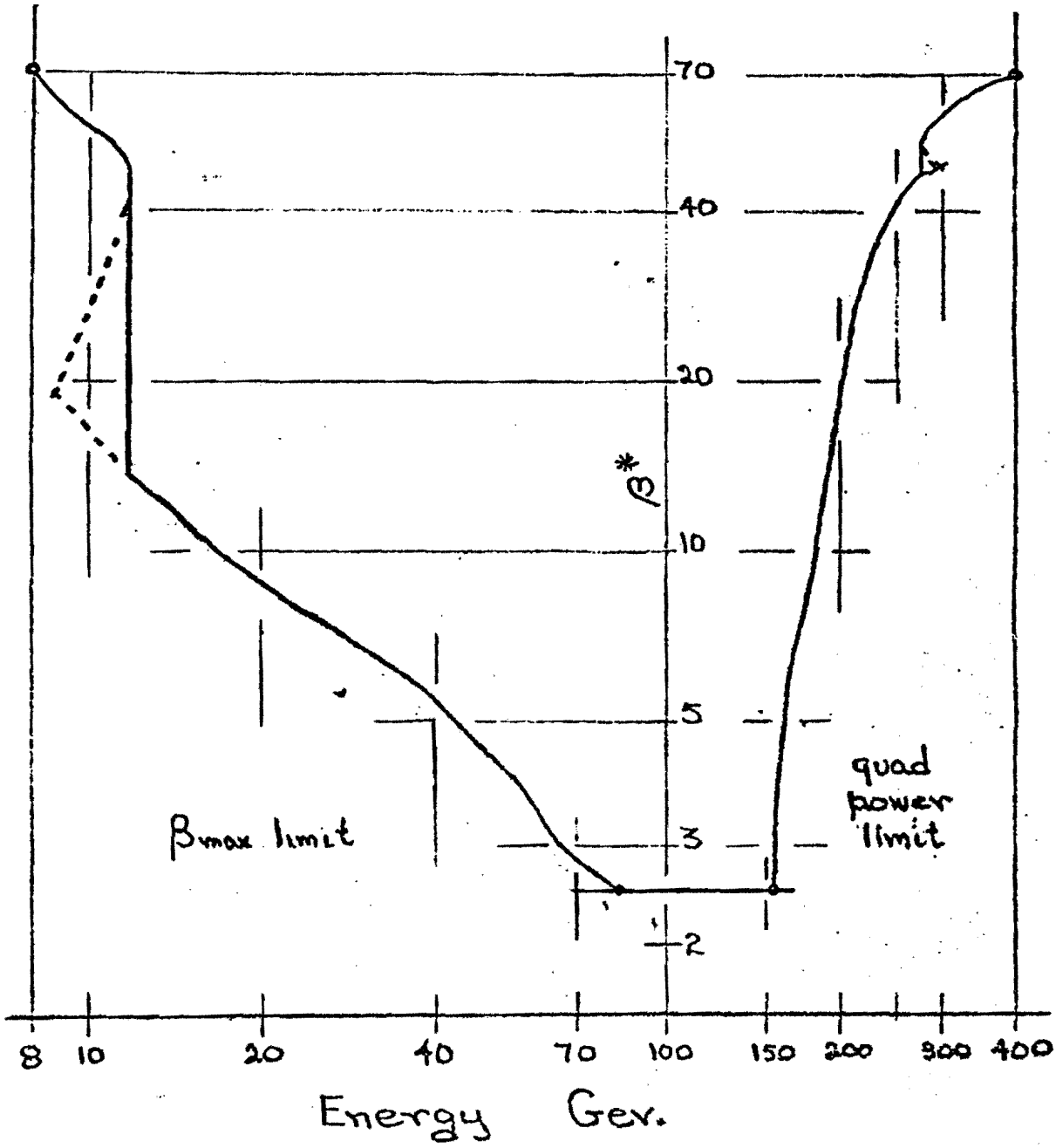

Figure 4. Minimum β^* vs. energy.

Fig. 3

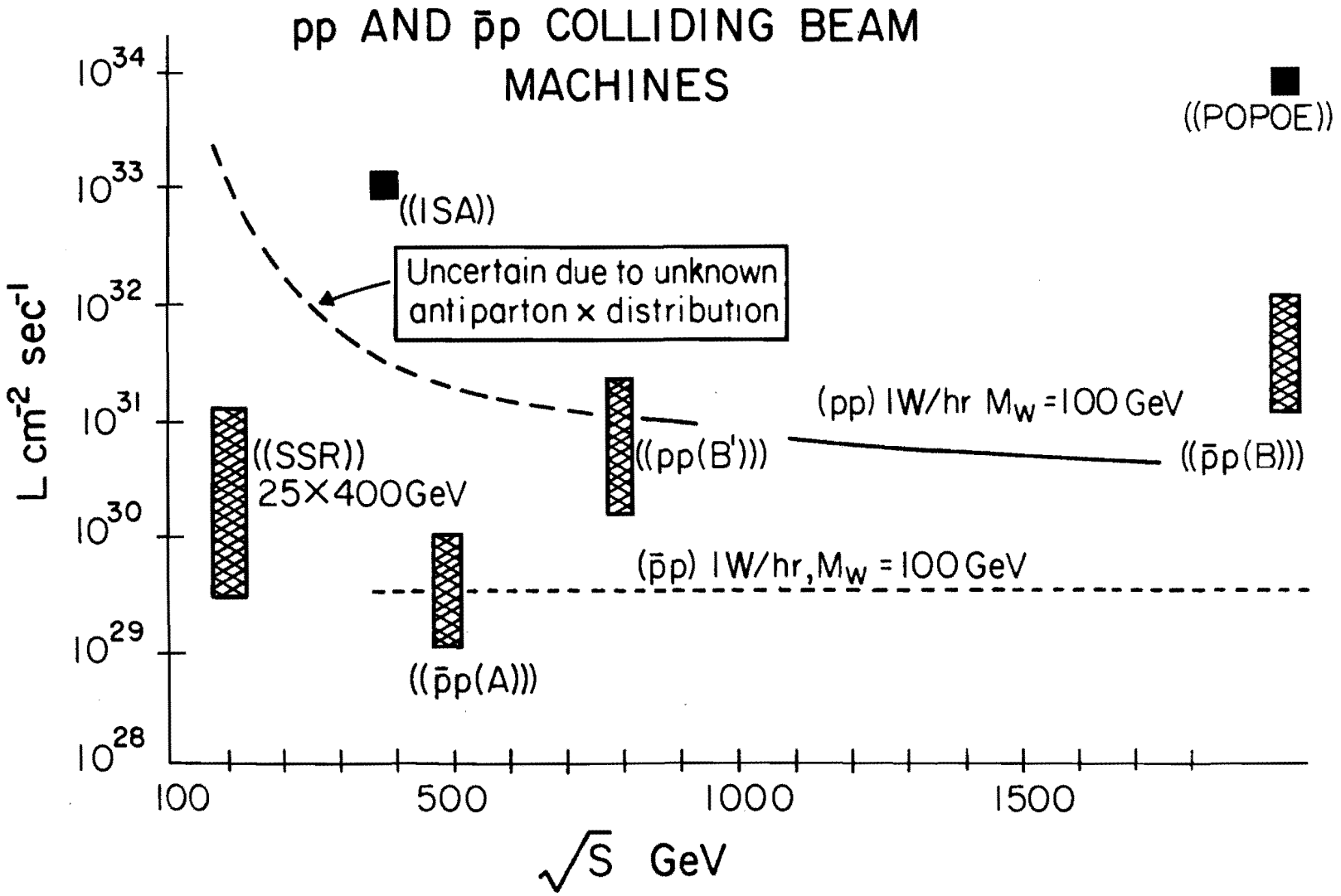
pp AND p̄p COLLIDING BEAM MACHINES
((POPOE))
((ISA))
Uncertain due to unknown antiparton x distribution
(pp) 1W/hr M_W = 100 GeV
((p̄p(B)))
((pp(B')))
((SSR))
25×400GeV
(p̄p) 1W/hr, M_W = 100 GeV
((p̄p(A)))
$L\ cm^{-2}\ sec^{-1}$
10^{34}
10^{33}
10^{32}
10^{31}
10^{30}
10^{29}
10^{28}
100
500
1000
1500
$\sqrt{S}$ GeV

Fig 14

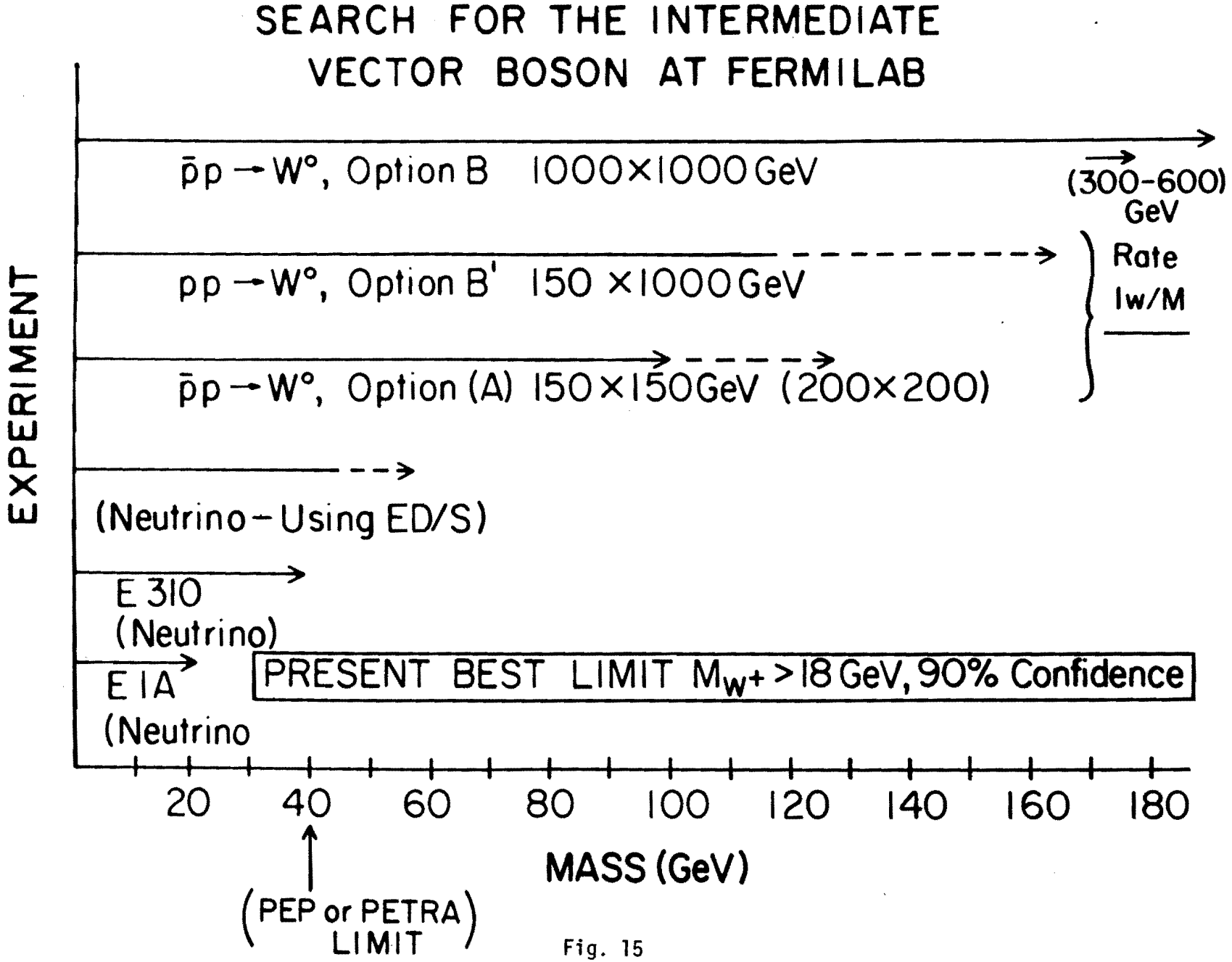
SEARCH FOR THE INTERMEDIATE VECTOR BOSON AT FERMILAB
EXPERIMENT
p̄p → W°, Option B 1000×1000 GeV
(300-600) GeV
pp → W°, Option B' 150 ×1000 GeV
Rate Iw/M
p̄p → W°, Option (A) 150×150 GeV (200×200)
(Neutrino – Using ED/S)
E 310 (Neutrino)
E 1A (Neutrino
PRESENT BEST LIMIT $M_{W^+} > 18$ GeV, 90% Confidence
20 40 60 80 100 120 140 160 180
MASS (GeV)
(PEP or PETRA LIMIT)

Fig. 15

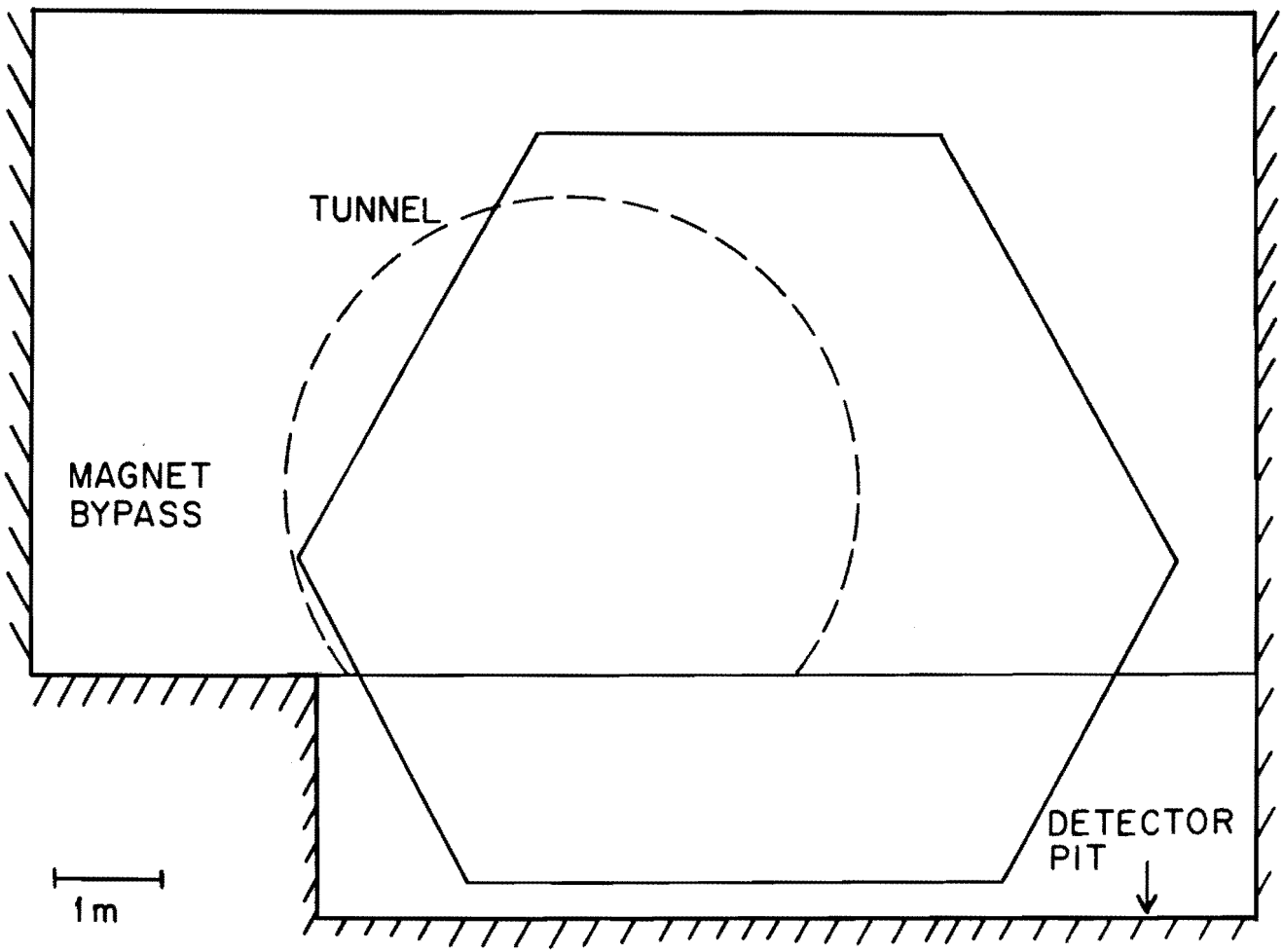

~4π ELECTRON-MUON DETECTOR

Fig 13